

The Effect of Electrode Polarity on Electrical Discharge Machining Performance in Water

Yoshiyuki UNO*, Toshikatsu NAKAJIMA* and Minoru OKADA*

(Received October 11, 1991)

SYNOPSIS

Practical utilization of ram type electrical discharge machining in unflammable fluid has been expected in place of inflammable kerosine type fluid for unmanned operation in a workshop. The electrical discharge machining performance in deionized water is experimentally investigated on the basis of the analysis of the crater generated by a single pulse discharge. The experimental analysis makes it clear that the electrical discharge machining performance in deionized water is greatly affected by the electrode polarity. The metal removal rate in the normal polarity machining is higher than that in reverse polarity machining, while the electrode wear rate in the normal polarity machining is greater than that in reverse polarity machining. Therefore the electrode polarity should be properly selected according to the purpose of machining.

1. INTRODUCTION

Ram type electrical discharge machining is conventionally performed in kerosine type fluid because of the electrode wear, surface finish, metal removal rate and so on. It is impossible to

* Department of Mechanical Engineering

operate the EDM machine without a man because of the danger of fire, though it is expected the whole day unmanned operation since the efficiency of electrical discharge machining is lower than that of other machining such as cutting or grinding. Therefore the unflammable fluid for ram type electrical discharge machining has been expected and a few reports on EDM in unflammable fluid have been published with copper electrode^{1), 2)}.

In this paper, from the above point of view, the possibility of utilization of deionized water for ram type EDM is experimentally investigated with graphite electrode which has recently been used for its good machinability. First the effect of the specific resistance on the electrical discharge phenomenon is investigated. Next the crater shape generated by a single pulse discharge is analyzed under the various discharge conditions. Furthermore the effect of electrode polarity on electrical discharge machining performance is discussed.

2. EXPERIMENTAL PROCEDURE

Fig.1 shows the schematic diagram of experimental apparatus of ram type electrical discharge machining used in this study. A single pulse discharge device is equipped in this apparatus. The electrode used in this test is graphite rod whose diameter is 5 mm. In case of a single pulse discharge experiment, the electrode is shaped to be conical whose vertical angle is about 40 degrees and nose radius about $10\mu\text{m}$. The workpiece is alloy tool steel SKD11 which is annealed and the surface of which is smoothly finished before each test to be less than $0.03\mu\text{m Ra}$. Deionized water whose specific resistance is about $1\text{M}\Omega\cdot\text{cm}$ is used as machining fluid. In the experiment of the effect of specific resistance, NaNO_3 is dissolved in the deionized water till the specific resistance reaches the setting value. The crater profile is investigated by the surface profile meter, the optical microscope, the scanning electron microscope(SEM), electron probe X-ray microanalyzer

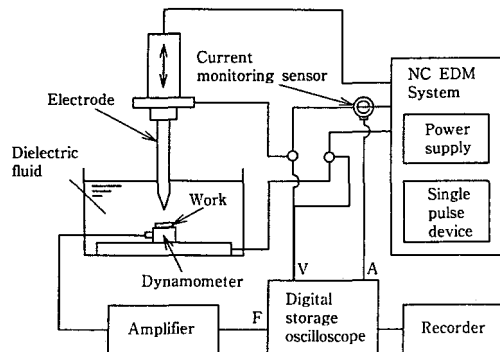


Fig.1 Schematic diagram of experimental apparatus with a single pulse discharge device

(EPMA) and so on. The discharge current and the impact force are measured by current monitoring sensor and piezoelectric dynamometer respectively.

Fig.2 shows a measured example of variation of gap voltage, discharge current and impact force in a single pulse discharge. The electrode approaches gradually the workpiece under the setting voltage E_0 . When the isolation of dielectric fluid is broken, an electric spark occurs. The gap voltage falls down to the discharge voltage $E_p(t)$ and the discharge current $I_p(t)$ appears simultaneously. Electrical discharge continues for presetting duration τ_p . The impact force, however, works only the short time from the beginning of the discharge³⁾. The discharge energy exhausted in a single pulse is expressed in the following equation;

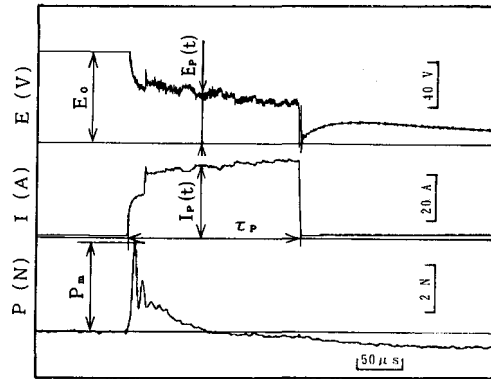


Fig.2 Variations of gap voltage, discharge current and impact force during a single pulse discharge

appears simultaneously. Electrical discharge continues for presetting duration τ_p . The impact force, however, works only the short time from the beginning of the discharge³⁾. The discharge energy exhausted in a single pulse is expressed in the following equation;

$$\varepsilon = \int E_p(t) \cdot I_p(t) dt$$

In this study, the condition of electrical discharge machining is set as follows;

Setting voltage: $E_0 = 120\text{V}(\text{constant})$

Discharge current: $I_p = 4\text{-}60\text{ A}$

Discharge duration: $\tau_p = 12\text{-}1000\ \mu\text{s}$

3. ANALYSIS OF A CRATER GENERATED BY A SINGLE PULSE DISCHARGE

3.1 The Effect of Specific Resistance of Water

Fig.3 shows the variation of the specific resistance of deionized water ρ with the passage of day when it is left in air. As shown in the figure, the specific resistance decreases rapidly at the early days and the rate of decrease becomes lower with the passage of day. It is considered that the deterioration of the specific resistance is due to the melting of CO_2 in air into the deionized water and the formation of CO_3^{2-} .

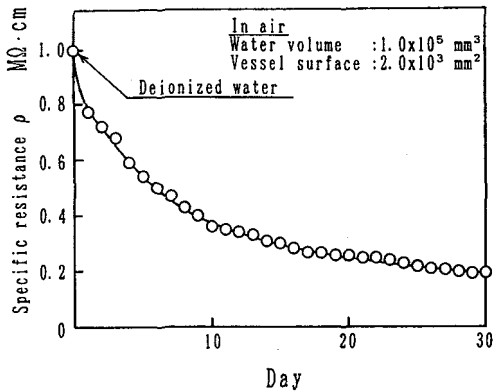


Fig.3 Variation of specific resistance of deionized water with time

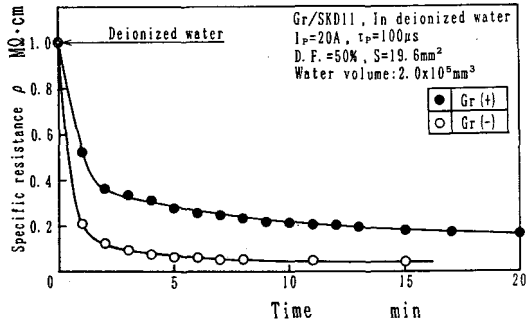


Fig.4 Variation of specific resistance of deionized water with the advance of EDM in a small vessel

Fig.4 shows the deterioration of the specific resistance of deionized water ρ with the advance of electrical discharge machining in a small vessel. The specific resistance decreases with the passage of time in both cases of electrode polarity. The rate of the decrease of specific resistance in normal polarity machining is higher than that in reverse polarity machining. This is due to the difference of chips produced during machining, because the metal removal rate in normal polarity machining is higher than that in reverse polarity machining as mentioned later.

As shown in these figures, the specific resistance of deionized water changes rapidly according to the condition, therefore the supervisory control of the specific resistance is needed in electrical discharge machining in water.

Fig.5 shows the relations between the crater diameter D_1 and the specific resistance ρ . As can be seen from the figure, the crater diameter increases with an increase of the specific resistance in normal polarity machining, while it doesn't change

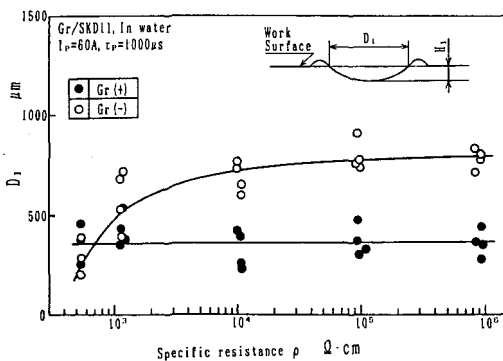


Fig.5 Relations between crater diameter D_1 and specific resistance ρ

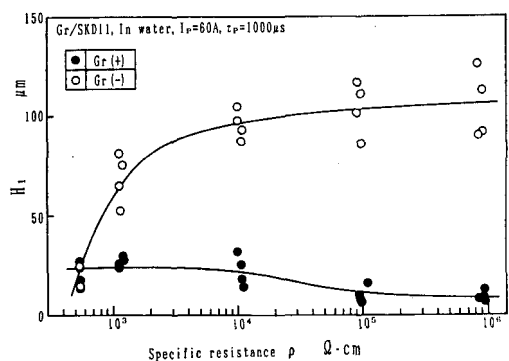


Fig.6 Relations between crater depth H_1 and specific resistance ρ

in reverse polarity machining.

FIG.6 shows the relations between the crater depth H_1 and the specific resistance ρ . The crater depth increases with an increase of the specific resistance in normal polarity machining. On the other hand, it has a tendency of decrease in reverse polarity machining.

As can be seen from these figures, it is considered that the stable machining is performed when the specific resistance of water is over $10^5 \Omega \cdot \text{cm}$. Therefore the following experiment is executed under the condition the specific resistance is $5 \times 10^5 - 1 \times 10^6 \Omega \cdot \text{cm}$. So far as the analysis of the crater shape generated by a single pulse discharge, reverse polarity discharge in deionized water seems to be inefficient as compared with normal polarity discharge.

3.2 The Effect of Machining Condition on the Crater Shape

Fig.7 shows the relations between the crater diameter D_1 and the discharge current I_p . As shown in the figure, the crater diameter increases with an increase of the discharge current in both cases of electrode polarity. The crater diameter in normal polarity machining is larger than that in reverse polarity machining.

Fig.8 shows the relations between the crater depth H_1 and the discharge current I_p . The crater depth in normal polarity machining increases with an increase of the discharge current, while it has a maximum value at $I_p = 20\text{A}$ and decreases with the discharge current in reverse polarity machining.

Fig.9 shows the relations between the crater diameter D_1 and the discharge duration τ_p . As can be seen from the figure, the

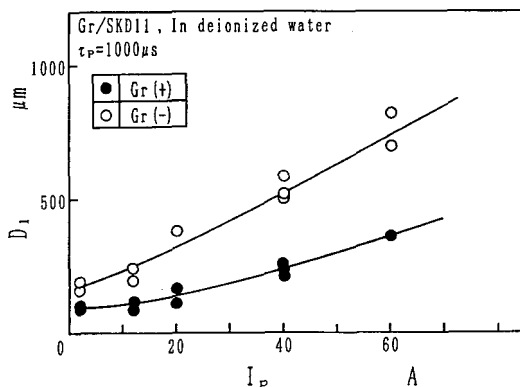


Fig.7 Relations between crater diameter D_1 and discharge current I_p

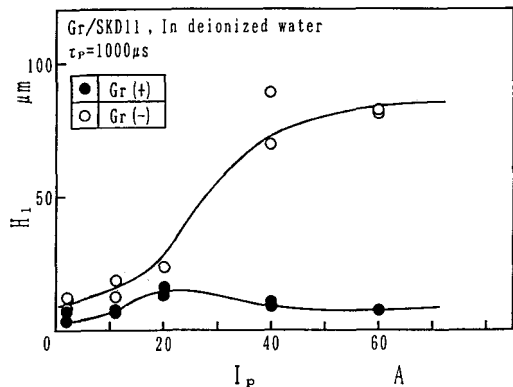


Fig.8 Relations between crater depth H_1 and discharge current I_p

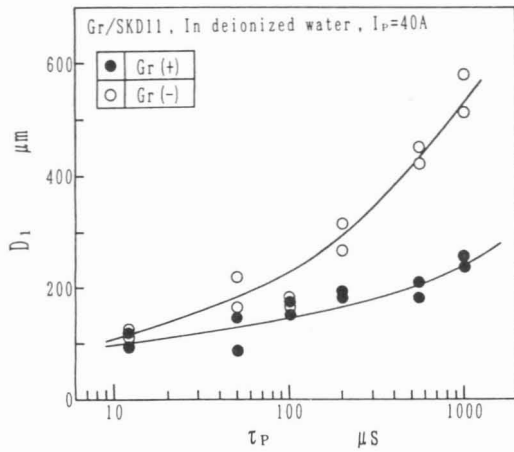


Fig.9 Relations between crater diameter D_1 and discharge duration τ_p

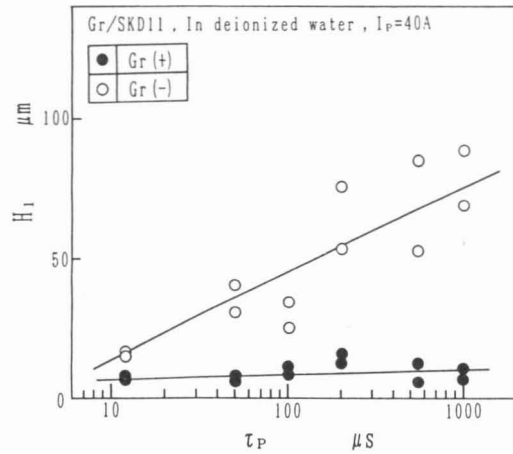


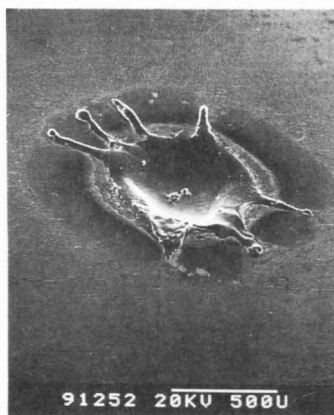
Fig.10 Relations between crater depth H_1 and discharge duration τ_p

crater diameter increases with an increase of the discharge duration in both cases of electrode polarity. The crater diameter in normal polarity machining is larger than that in reverse polarity machining.

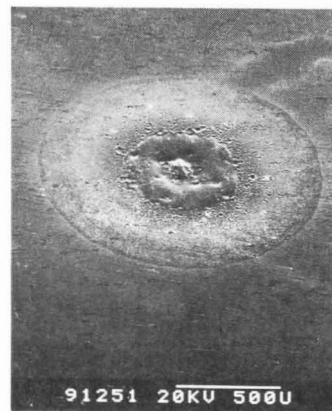
Fig.10 shows the relations between the crater depth H_1 and the discharge duration τ_p . The crater depth in normal polarity machining increases with an increase of the discharge duration τ_p , while it is approximately kept constant in reverse polarity machining.

3.3 The Difference of the Crater due to the Electrode Polarity

Fig.11 and 12 are the SEM photographs which show the difference of the crater shape due to the electrode polarity under the same machining condition. As shown clearly in these figures,



Gr(-)/SKD11



Gr(+)/SKD11

Fig.11 SEM photographs of crater ($I_p = 60A$, $\tau_p = 1000\mu s$)

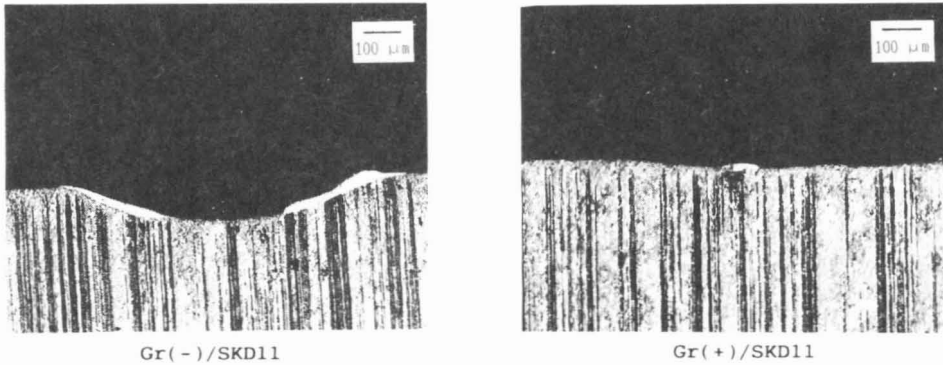


Fig.12 SEM photographs of crater section ($I_p = 60A$, $\tau_p = 1000\mu s$)

the crater shapes in two electrode polarity differ remarkably. That is, the crater diameter and the depth in normal polarity machining are larger than those in reverse polarity machining, while the heat affected zone seems approximately to be the same size in both cases. That is due to the imbalance of energy distribution, because the total energy exhausted during a single pulse discharge is equal in both cases of electrode polarity.

Fig.13 shows the relations between the maximum impact force P_m which operates the workpiece during a single pulse discharge and the discharge current I_p . As shown in the figure, the maximum impact forces in both cases are approximately the same value. This shows that the difference between two polarities are not due to the impact force. Then it is considered that the difference between two polarities is due to the heat energy given to the workpiece during a single pulse discharge.

Fig.14 shows the relations between the melting volume of

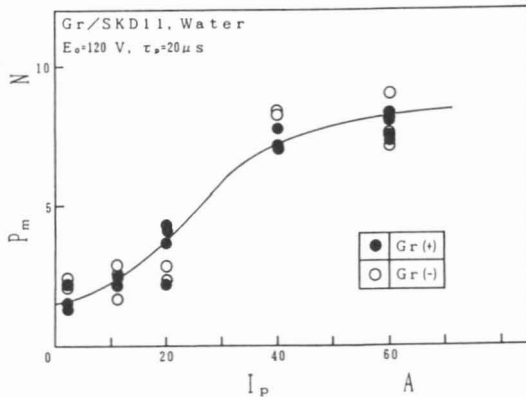


Fig.13 Relations between the maximum impact force P_m and discharge current I_p

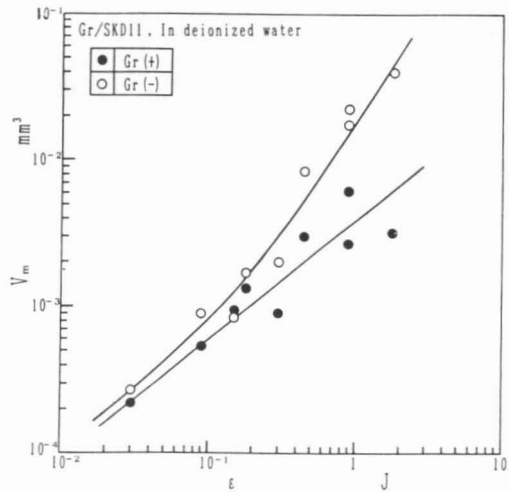


Fig.14 Relations between melting volume V_m and discharge energy ϵ

crater V_m and the discharge energy ϵ . The melting volume of crater is calculated by the following equation³⁾;

$$V_m = (1/6) \pi H_m \{3(D_m/2)^2 + H_m^2\}$$

As shown in this figure, the melting volume of crater increases with an increase of the discharge energy. The melting volume of crater in normal polarity machining is larger than that in reverse polarity machining. This shows that the difference between two polarities is due to the heat energy.

Fig.15 is the SEM photographs which show the electrode wear in both cases of electrode polarity. As can be seen from these photographs, the electrode shapes differ remarkably between two polarities. The wear in normal polarity machining is much larger than that in reverse polarity machining. It seems that the wear in normal polarity machining is due to the crack propagation resulting from rapid heat cycle, because the surface resembles closely to the fracture surface of graphite.

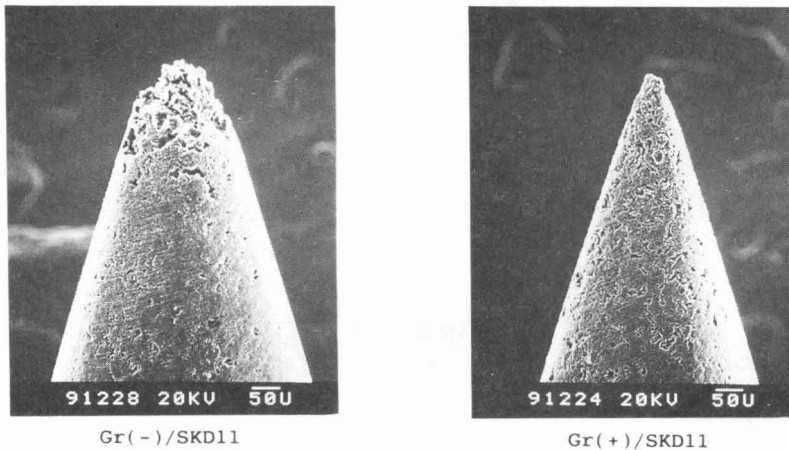


Fig.15 SEM photographs of graphite electrode after discharge
($I_p = 60A$, $\tau_p = 1000\mu s$)

4. ELECTRICAL DISCHARGE MACHINING PERFORMANCE IN WATER

Fig.16 shows the relations between the metal removal rate \dot{R} and the discharge duration τ_p for various discharge current I_p . The metal removal rate increases with an increase of the discharge current. In normal polarity machining, the metal removal rate has a maximum value at the discharge duration $\tau_p = 200 \mu s$ for $I_p = 12-60 A$. On the other hand, the metal removal rate in reverse

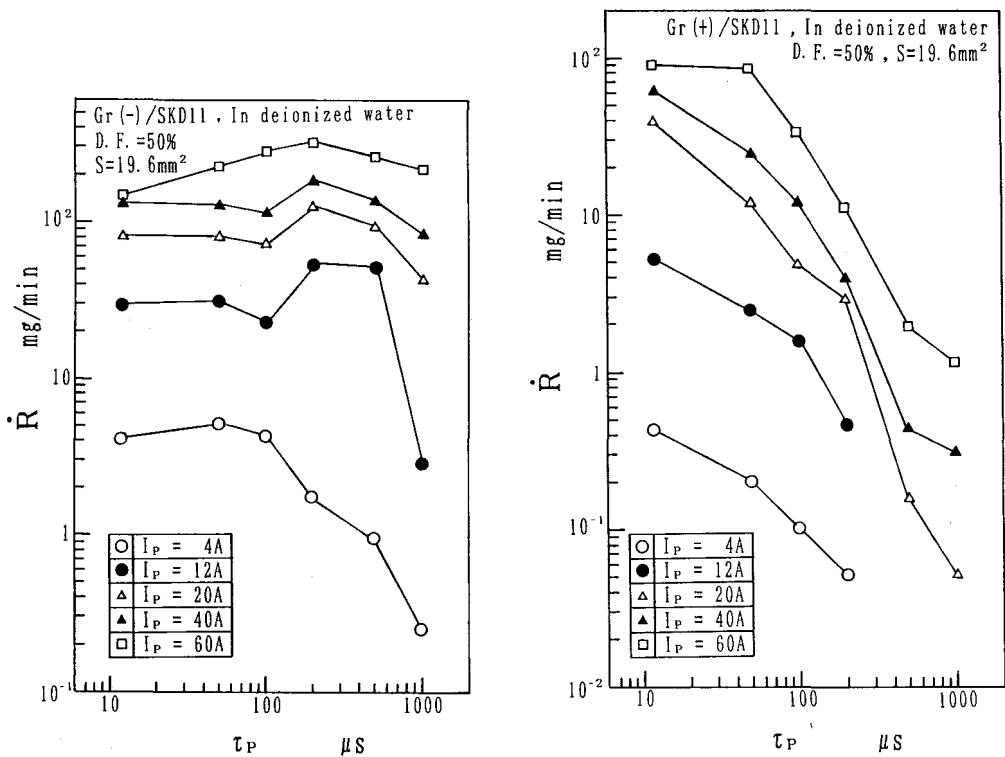


Fig.16 Relations between metal removal rate \dot{R} and discharge duration τ_p ,

polarity machining is smaller than that in normal polarity machining and decreases with an increase of the discharge duration.

Fig.17 shows the relations between the electrode wear rate W and the discharge duration τ_p , for various discharge current. It can be seen from the figures that the electrode wear rate increases with an increase of the discharge current but it doesn't change for the variation of discharge duration except for $I_p = 4A$. On the other hand, the electrode wear rate in reverse polarity machining is less than that in normal polarity machining in the range of higher discharge current and shorter discharge duration.

Fig.18 shows the relations between the electrode wear rate W and the metal removal rate \dot{R} . The electrode wear rate decreases with an increase of the metal removal rate in both cases. In the range of higher metal removal rate, the electrode wear rate in reverse polarity machining is lower than that in normal polarity machining. However it should be noted that the metal removal rate in reverse polarity machining under the same condition is lower than that in normal polarity machining as shown in Fig.16. Therefore the electrode polarity should be selected according to the purpose of machining.

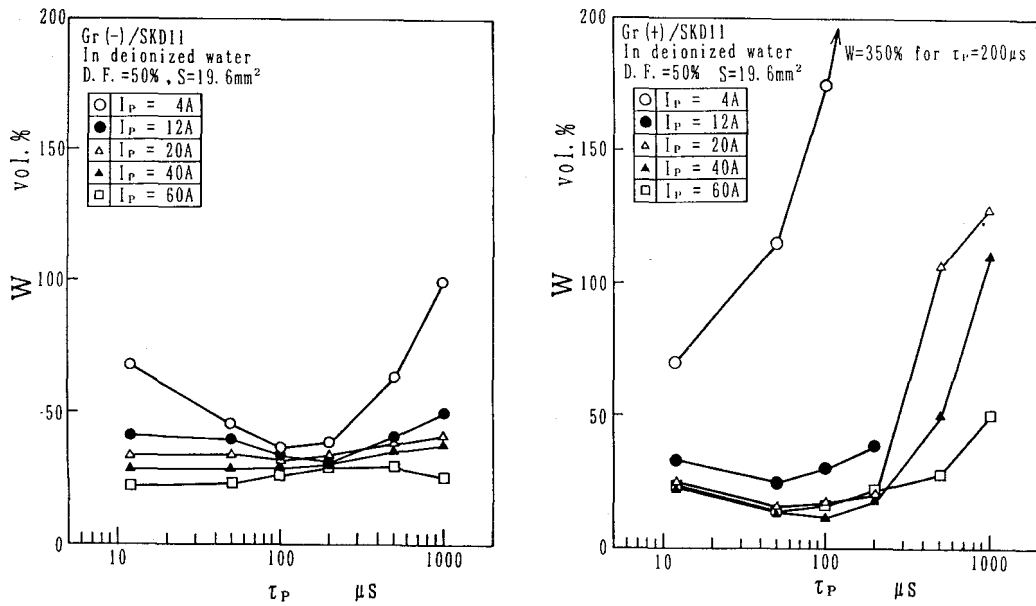


Fig.17 Relations between electrode wear rate W and discharge duration τ_p

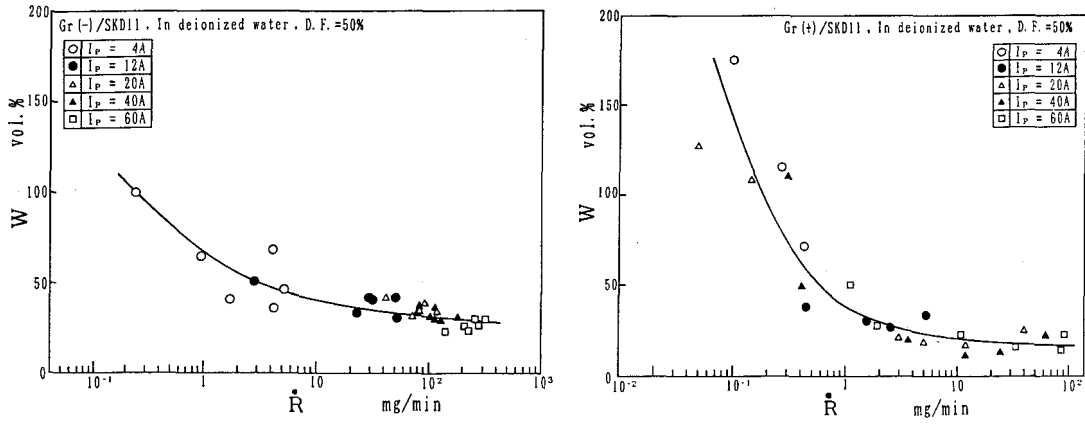


Fig.18 Relations between electrode wear rate W and metal removal rate \dot{R}

Fig.19 are SEM photographs showing the electrode surface after machining in both cases. Many metal fragments are stuck to the electrode surface in reverse polarity machining. On the other hand, only a few spherical chips are observed among the porous surface layer of electrode.

Fig.20 shows the results of elementary analysis of the same size electrode surface in both cases of electrode polarity. More intensity of workpiece components are detected in reverse polarity machining. It is considered that the less wear of electrode in reverse polarity machining as compared with that in normal polarity

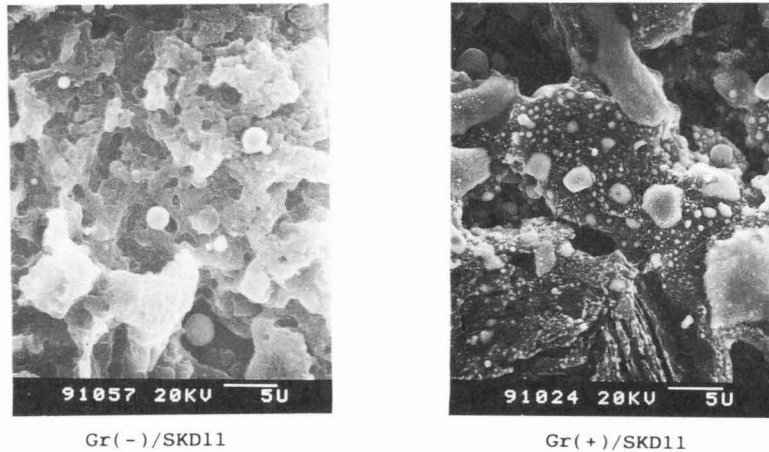


Fig.19 SEM photographs of electrode surface after machining
($I_p = 20A$, $\tau_p = 100\mu s$)

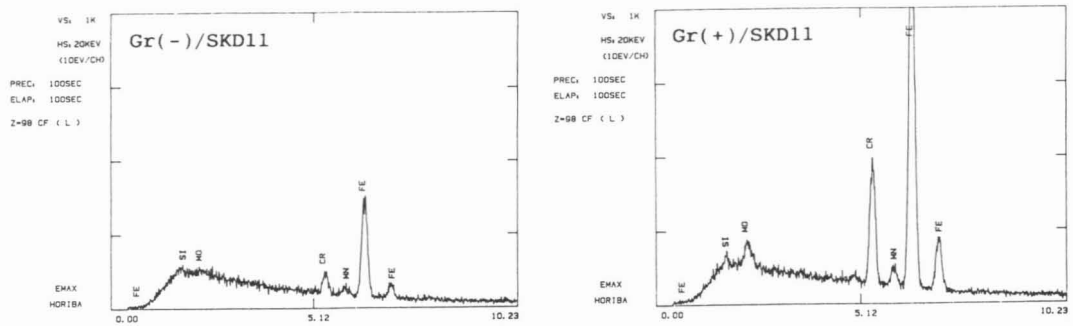


Fig.20 Results of elementary analysis of electrode surface

machining is due to the coating of metal on the surface of electrode.

5. CONCLUSIONS

The effect of electrode polarity on the electrical discharge machining performance in water is experimentally investigated on the basis of the analysis of a crater shape generated by a single pulse discharge. Main conclusions obtained are as follows:

- (1) The specific resistance of water used in discharge machining is needed to be over $10^5 \Omega \cdot \text{cm}$.
- (2) The melting volume of a crater in normal polarity discharge is larger than that in reverse polarity discharge.
- (3) The metal removal rate in normal polarity machining is higher, while the electrode wear rate is larger.

(4) When compared at the same metal removal rate, the electrode wear rate in reverse polarity machining is smaller than that in normal polarity machining.

(5) The electrode surface in reverse polarity machining is covered with many metal fragments.

REFERENCES

- 1) Y.KIMOTO and K.TAMIYA: Journal of the Japan Society of Electrical Machining Engineers, Vol.3, No.5(1969)23.
- 2) T.MASUZAWA: Journal of the Japan Society of Electrical Machining Engineers, Vol.14, No.27(1980)50.
- 3) Y.UNO, O.ENDO and T.NAKAJIMA: Journal of the Japan Society of Electrical Machining Engineers, Vol.25, No.49(1991)9.